Demodulation of White-Light Interferometry Based on Variable Sampling Length Fourier Transform

Xie Jiehui Wang Fuyin Hu Zhengliang Hu Yongming

(*College of Optoelectronic Science and Engineering, National University of Defense Technology, Changsha, Hunan* 410073, *China*)

Abstract The Fourier transform (FT) method for demodulating the extrinsic Fabry-Perot interferometer (EFPI) possesses the advantage of high resolution and wide dynamic range for the absolute measurement in demodulating white-light EFPI. However, the dynamic range and the resolution of this method are limited by the nonlinear relationship with the scanning wavelength and the fence effect of FT, respectively. The cubic spline interpolation and a modified FT algorithm are used to reduce the influence of chirped spectrum and increase the resolution, respectively. The simulation and the experimental results show that the algorithm has seventy times enhancement of the resolution of demodulation.

Key words sensors; high resolution; new algorithm; EFPI

OCIS codes 040.1880; 200.4560; 310.6845

基于变采样长度傅里叶变换的白光干涉仪解调

谢杰辉 王付印 胡正良 胡永明

(国防科技大学光电科学与工程学院, 湖南 长沙 410073)

摘要 基于傅里叶变换的非本征光纤法布里-珀罗干涉仪(EFPI)的解调方法,对解调白光干涉的 EFPI 具有解调精度高,动态范围大,且可实现腔长的绝对测量等优点。然而,该方法的动态范围和解调精度分别受限于采样导致的非线性谱分布以及傅里叶变换的栅栏效应。分别采用三次样条插值和改进的傅里叶变换来消除光谱的啁啾特性和提高解调精度。仿真和实验证明该算法的解调精度提高了 70 倍。

关键词 传感器; 高精度; 新型算法; 非本征光纤法布里-珀罗干涉仪

中图分类号 TN253 **文献标识码** A **doi**: 10.3788/AOS201434.s106009

1 Introduction

Fiber optic sensors have various advantages, such as small size, large dynamic range, high sensitivity, immunity to electromagnetic interference, resistance to harsh environment and capability of multiplexing[1]. In the past decades, extrinsic Fabry-Perot interferometer (EFPI) had emerged its development potential. Lots of important parameters can be measured by EFPI, including pressure, temperature, sound and so on. In order to improve resolution of EFPI, numerous methods had been proposed, including Fourier transform (FT)[2-3], wavelength-tracking[4], two-peak wavelength interrogation[1], cross-correlation algorithm[5-6], minimum mean square error estimation (MMSE)[7], integrating a data preprocessed FT, and the MMSE-based signal processing[8]. Above that, the FT method has a resolution not better than tens of micron dimension because of the fence effect. The method of fast FT[2] was reported in 2000. The method of using the data processing technology of Gaussian interpolation in frequency domain has two times enhancement of resolution. The method of reducing the influence of nonlinear wavelength sampling showed an enhancement of resolution about three times in 2013[9].

In this paper, a new signal-processing algorithm is described based on frequency estimation of the spectrogram of single-mode EFPI under white-light illumination. We change the sampling length of FT and the frequency distribution is not the integer values anymore, the result shows that this signal processing

收稿日期: 2014-01-22; **收到修改稿日期**: 2014-02-25

作者简介: 谢杰辉(1990—),男,硕士研究生,主要从事光纤传感方面的研究。E-mail: xjh199002@sina.com

导师简介: 胡永明(1960—),男,教授,博士生导师,主要从事光纤传感及光纤激光器等方面的研究。E-mail: sdss@12cn.com (通信联系人)

technology has an enhancement of resolution of demodulation about seventy of times.

2 Theory

The simple FFT method was used to demodulate the main frequency of the signal in wavelength-domain, while the digital frequency is not a constant but a chirp spectrum. For a low finesse F-P interferometer, the reflected optical intensity can be expressed as:

$$I_r(\lambda_n) = A(\lambda_n) + B(\lambda_n)\cos\left(\frac{4\pi d}{\lambda_n} + \pi\right) = A(\lambda_n) + B(\lambda_n)\cos\left(2\pi\frac{2d}{\lambda_n^2}\lambda_n + \pi\right), \quad (1)$$

where d is the cavity length, $A(\lambda_n)$ is the background introduced by the light source; $B(\lambda_n)$ is the contrast that is relevant to the reflection of the fiber ends; π is introduced by the reflection of the second reflector of the EFPI; λ_n is the wavelength. $I_r(\lambda_n)$ shows that the frequency of interferometric fringe changes with λ, the interference spectrum acquired by the spectrometer is equal to that of the interval sampling in wavelength domain, and the frequency $1/\lambda_n^2$ represents chirp spectrum, which causes an expansion of the basic frequency bandwidth with the increase of cavity length, and could lead to a decrease of the dynamic range. We change the signal from wavelength domain to optical frequency domain as

$$I_r(\lambda_n) = A(\lambda_n) + B(\lambda_n)\cos\left(\frac{4\pi d}{\lambda_n} + \pi\right) = A(\lambda_n) + B(\lambda_n)\cos\left(\frac{4\pi d\upsilon}{c} + \pi\right), \quad (2)$$

where the frequency $2d/c$ is a constant, however, optical frequency $\nu = c/\lambda$ is not a linear variable. In order to reduce errors caused by this effect, the cubic spline interpolation is used to resample the interference spectrum and the new spectrum is equally sampled in the frequency domain. The new spectrum after eliminating the influence of light source is shown as

$$I = 1 + \cos\left(\frac{4\pi d\upsilon}{c} + \pi\right). \quad (3)$$

The new spectrum in digital frequency domain can be expressed by FT method as

$$F(\mathrm{j}\Omega) = \int_{-\infty}^{+\infty} I\exp(-\mathrm{j}\Omega\upsilon)\,\mathrm{d}\upsilon = \int_{-\infty}^{+\infty}\left(1-\cos\frac{4\pi\upsilon d}{c}\right)\exp(-\mathrm{j}\Omega\upsilon)\,\mathrm{d}\upsilon = \pi\left[2\delta(\Omega) - \delta\left(\Omega+\frac{4\pi d}{c}\right) - \delta\left(\Omega-\frac{4\pi d}{c}\right)\right], \quad (4)$$

where Ω is the angular frequency. According to the discrete FT (DFT)[10], the new spectrum $I(n)$ can be transformed to the frequency:

$$I(m) = \sum_{n=0}^{N-1} I(n)\exp(-\mathrm{j}2\pi nm/N), \quad (5)$$

where m, n, N, $I(m)$ represent the order of digital frequency, the order of wavelength, the sampling length of light frequency domain, and the amplitude of different frequencies, respectively. Traditionally, $m = 0,1,\cdots,N-1$, and $n = 0,1,\cdots,N-1$.

The cavity length of the F-P cavity can be expressed as

$$d = \frac{ck_{\mathrm{d}}}{2N\delta\upsilon}, \quad (6)$$

where $\delta\upsilon = (c/\lambda_1 - c/\lambda_N)/(N-1)$ is the sampling interval of optical frequency; c is the light speed in vacuum; k_{d} is the subscript for the peak of the frequency spectrum. In our experiment, N = 512 and $\delta\upsilon$ = 21 GHz. Because the result of k_{d} can only be the integer values, the ideal resolution is $\Delta d = c/(2N\delta\upsilon) \approx 13.8$ μm, hence that the parameter N and $\delta\upsilon$ are limited by the hardware, the only parameter we can change is k_{d}.

In this paper, we reduce one sampling point of the DFT gradually when we proceed one DFT calculation to reduce the fence effect and improve the resolution. When N is reduced to N_i, the distribution of m changes with N_i, $m = 0, N/N_i, 2N/N_i, \cdots, N-1$, and $n = 0,1,\cdots,N_i-1$, the final result shows that the k_{d} is not the integer values but the decimal number, and there has more than one point in the range of 1 Hz (shown in Fig. 2), so the resolution has a significant improvement.

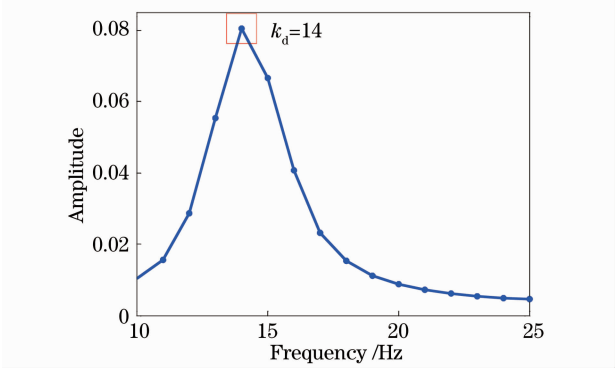

Fig. 1 Results of FFT

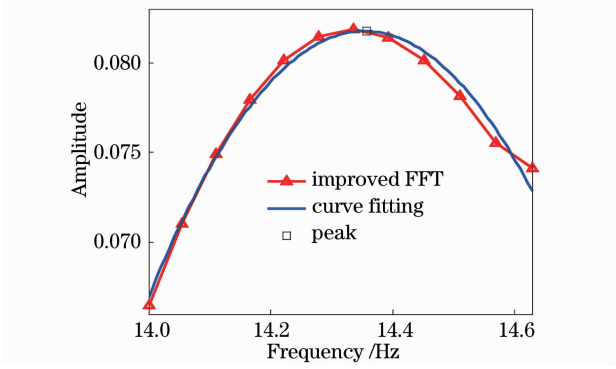

Fig. 2 Subdivision of the peak

We can express the theory as

$$I(m_i) = \frac{N}{N_i}\sum_{n=0}^{N_i-1} I(n)\exp(-\mathrm{j}2\pi nm_i/N_i), \quad (7)$$

where $m_i - m_{i-1} = N/Ni \geqslant 1$, N_i ranges 0.9N to N. The result shows that there are several points between

1Hz with the change of Ni (shown in Fig. 2). Different frequencies have different amplitudes, and the peak frequency corresponds to the most precise frequency.

Fig. 2 is the subdivision of the peak in Fig. 1. The resolution of frequency is only 1 Hz in Fig. 1, which means that the resolution of cavity length is only 13.8 μm. The resolution of frequency is 0.05 Hz in Fig. 2, which means that the resolution of cavity length is up to 0.7 μm. And the result is that the resolution has nearly twenty times improvement.

The two order polynomial curve fitting is used to ensure the more precise basic frequency of the reflected signal, which is shows in Fig. 2, marked by '△'; and the black square is the more precise value of k_d. After a series of signal processes, a resolution improvement of seventy times is obtained.

3 Experiment

The experimental setup is shown in Fig. 3. The fiber Bragg grating interrogation analyzer (FBGA) offers a broadband source with a full-width at half-maximum (HMFW) of 45 nm, and a peak wavelength of 1540 nm. Its time sampling rate is 5000 Hz and the wavelength sampling length is 512. The Michelson interferometer is used to represent the low finesse EFPI. And the step motor stage is used to change the air gap. The reflected optical intensity is shows in Fig. 4.

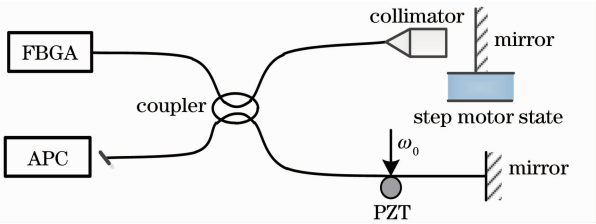

Fig. 3 Diagram of the experimental setup

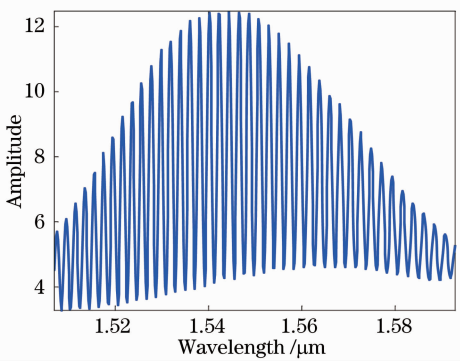

Fig. 4 Reflect optical intensity

In the experiment, we change the air gap by step motor stage with precision of 1 μm. To avoid the influence of environment, a fast signal collection is used in this system by FBGA. The demodulation results are shown in Figs. 5 and 6.

Figures 5 and 6 are the outcome of method 1 and method 2, respectively (where method 1 and method 2

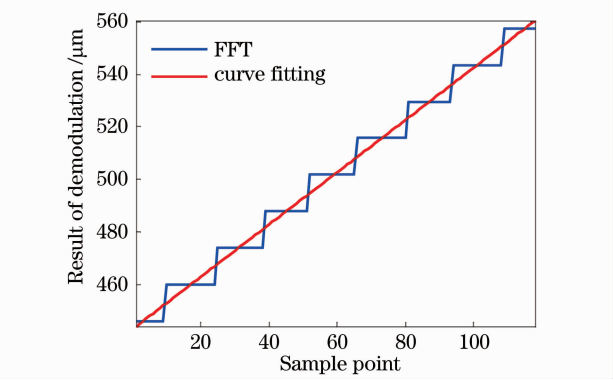

Fig. 5 Demodulation of method 1

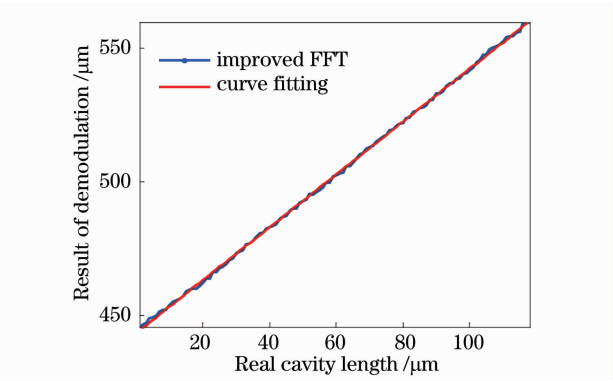

Fig. 6 Demodulation of method 2

represent the simple FFT after interpolation in optical frequency and the new algorithm respectively). The result shows that the new algorithm has an obvious improvement in the resolution of cavity length. And the residual mean square of method 1 and method 2 are 1.58×10^{-11} and 3.8×10^{-13}, respectively. Obviously, the resolution has a considerable melioration.

Furthermore, a sensitive EFPI was used to detect the change of pressure. In the experiment, the sensor (EFPI) was put in a water tank, and the depth of the EFPI is controlled manually. Figure 7(a) shows the structure of the EFPI and the experimental setup and Fig. 7(b) shows the structure of the EFPI.

Figure 8 shows the cavity length changes with the water level. We know that the water pressure is proportional to the water level, and the experimental result shown in Fig. 8 proves that the EFPI shows an excellent linear relationship between the cavity length and the pressure, the sensitivity of the sensor is nearly 3 nm/Pa. The deviation of demodulation, including the error of depth and the error of the algorithm, is shown in Fig. 9.

Finally, the EFPI was put under water statically to detect its stability. Figure 10 shows the experimental result. The cavity length was measured for 3000 s, and the sampling rate is 1 sample/s. In Fig. 10, the standard deviation (SD) is 0.2 μm, which means that, compared and method 1, the resolution of method 2 has seventy times improvement.

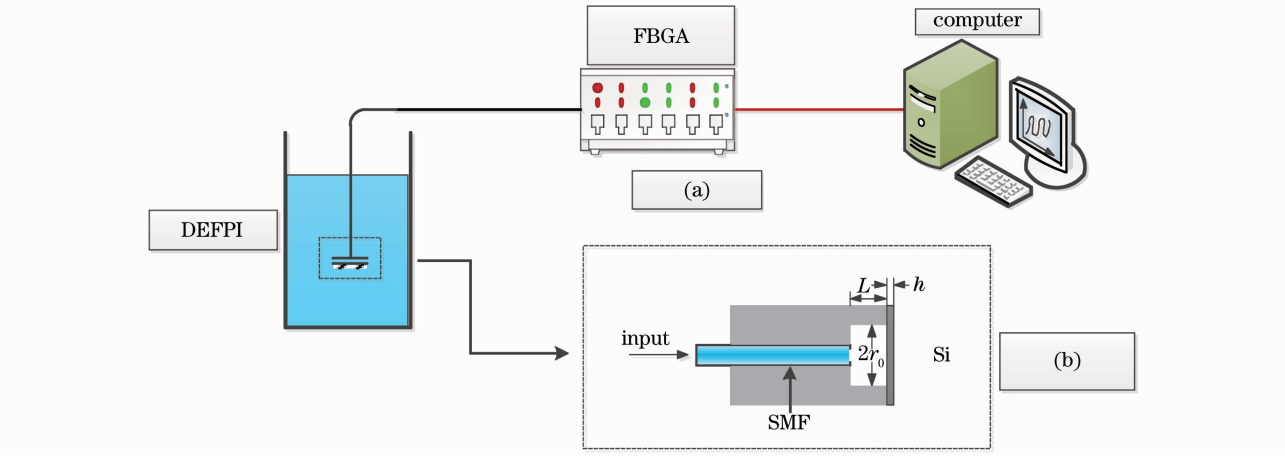

Fig. 7　Diagram of the experimental setup. (a) Experimental setup; (b) structure of the EFPI

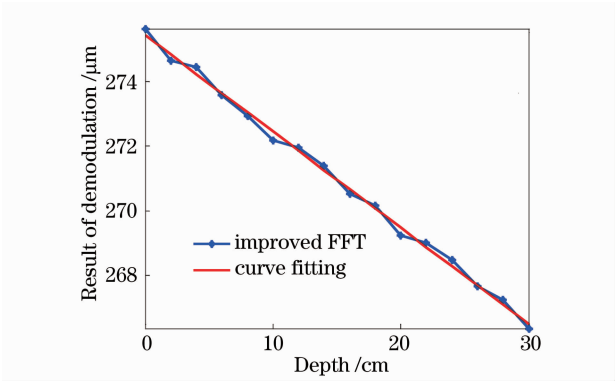

Fig. 8　Cavity changes with the water level

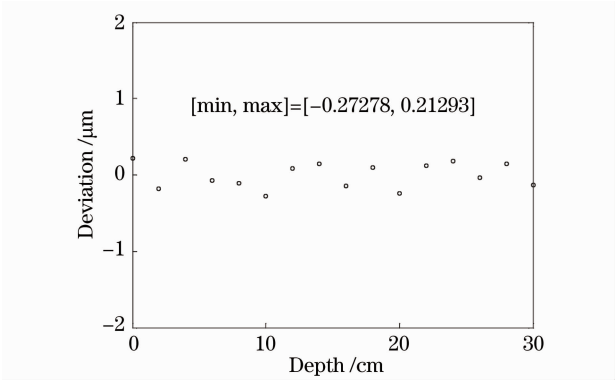

Fig. 9　Deviation of the fitting line and the detect points

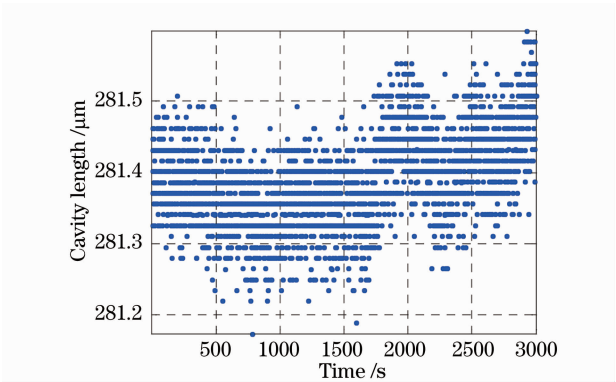

Fig. 10　Experimental results for stability of EFPI

4　Conclusion

In conclusion, we propose and experimentally verify a new algorithm for demodulating the F-P cavity length. The experimental result shows that the resolution of the demodulation has a remarkable promotion by using the new algorithm. In addition, the resolution of cavity length will be influenced by the stability of the system. The new algorithm has many applications potentially in temperature and pressure measurement.

Reference

1 Wang A, Xiao H, May R G, *et al*.. Optical fiber sensors for harsh environments[C]. International Society for Optics and Photonics, 2000.

2 Liu T, Fernando G F. A frequency division multiplexed low-finesse fiber optic Fabry-Perot sensor system for strain and displacement measurements[J]. Review of Scientific Instruments, 2000, 71(3): 1275 - 1278.

3 Jiang Y. Fourier transform white-light interferometry for the measurement of fiber-optic extrinsic Fabry-Perot interferometric sensors[J]. IEEE Photon Technol Lett, 2008, 20(2): 75 - 77.

4 Qi B, Pickrell G R, Xu J, *et al*.. Novel data processing techniques for dispersive white light interferometer[J]. Opt Eng, 2003, 42(11): 3165 - 3171.

5 Zhenguo Jing, Qingxu Yu. White light optical fiber EFPI sensor based on cross-correlation signal processing method[C]. Proc 6th Symp Test and Measurement, 2005.

6 Wang W, Li F. Large-range liquid level sensor based on an optical fibre extrinsic Fabry-Perot interferometer[J]. Opt & Lasers in Eng, 2014, 52: 201 - 205.

7 Song Shide. Study on the Characteristics and Sensing Applications of Long Period Fiber Gratings[D]. Dalian: Dalian University Technology, 2006.
宋世德. 长周期光纤光栅的特性及传感应用研究[D]. 大连: 大连理工大学, 2006.

8 Yu Q, Zhou X. Pressure sensor based on the fiber-optic extrinsic Fabry-Perot interferometer[J]. Photon Sensors, 2011, 1(1): 72 - 83.

9 Wang Z, Jiang Y, Ding W, *et al*.. Fourier transform white-light interferometry based on nonlinear wavelength sampling[J]. Opt Eng, 2013, 52(10): 104102.

10 Ni Xiaoqi, Wang Ming, Chen Xuxing, *et al*.. Quasi-distributed measurement of optical fiber MEMS Fabry-Perot pressure sensors[J]. J Nanjing Normal University: Engineering and Technology Edition, 2009, 9(4): 82 - 86.
倪小琦, 王　鸣, 陈绪兴, 等. 光纤 MEMS 法布里-珀罗压力传感器的准分布式测量[J]. 南京师范大学学报: 工程技术版, 2009, 9(4): 82 - 86.

栏目编辑: 何卓铭